Journal of Power Sources 253 (2014) 27–34

Contents lists available at ScienceDirect

Journal of Power Sources

journal homepage: www.elsevier.com/locate/jpowsour

Size effect of nickel oxide for lithium ion battery anode

Ming-Yao Cheng*, Yun-Sheng Ye, Tse-Ming Chiu, Chun-Jen Pan, Bing-Joe Hwang*

Department of Chemical Engineering, National Taiwan University of Science and Technology, 43, Sec. 4, Keelung Rd., Taipei 10607, Taiwan, ROC

HIGHLIGHTS

- The originally NiO nanostructured electrode is able to reduce the voltage hysteresis loop.
- The 3-D porous nanostructure of NiO remains stable during charge discharge process.
- The *I*–*V* characteristic indicates the high redox reaction kinetics.
- The anomalous high capacity is contributed by the reversible SEI layer.
- The charge discharge energy efficiency can be much improved.

ARTICLE INFO

Article history:
Received 20 September 2013
Received in revised form
7 December 2013
Accepted 10 December 2013
Available online 18 December 2013

Keywords:
Size effect
Nickel oxide
Anode
Lithium ion battery
Conversion reaction

ABSTRACT

In this study, size effect of NiO particles has been studied as the anode material of lithium ion battery. It is found that NiO nanoparticles synthesized in confined space of ordered mesoporous silica behave anomalous high capacity and higher energy efficiency than sub-micro-sized NiO does. The higher energy efficiency is resulted from the reduction of the hysteresis loop between charge and discharge voltage plateaus, the main drawback of conversion reaction-based metal oxide anode materials. The interesting behavior is proposed to be the reversible formation/dissolution of solid electrolyte interphase (SEI) layers associated with 3-D porous, originally nanostructured NiO electrode that is able to remain stable during charge–discharge process.

1. Introduction

Nowadays the requirements of next generation Lithium ion battery need higher energy density, larger specific capacity, better stability and larger temperature operation window. Regarding the progress of next generation anode materials, several Li storage mechanisms, for example, intercalation (graphite), Li-metal alloying, and conversion reaction (Li + metal oxide → LiO + nano-sized metal), have been reported [1–9]. Nevertheless, the novel materials are able to deliver capacities several times higher than that of conventional graphite. However, different materials lead to different challenges that are awaiting solutions. Transition metal oxides, discovered by Tarascon et al. in 2000 [4], show a specific capacity of 2–3 folds to that of commercially adopted graphite (372 mAh g^{-1}). Nevertheless the conversion reaction shows large hysteresis loop between charge and discharge voltage plateau, indicating its low energy efficiency [10–14]. Some studies employ nanostructured metal substrate as current collectors for better performance, however, the results does not show obvious improvement in the reduction of hysteresis loop [13,15].

Considering the details of conversion reaction at 1st charge process, large-sized metal oxide is able to be reduced to form internally nanostructured metals at a relatively low potential than the subsequently charge steps. During charging step, the low-density Li_2O is formed in the matrix, resulting in dispersion of the nanostructured metals in Li_2O matrix. In the discharge process, the electron transfer needs to go through the Li_2O matrix to access the nanostructured metals. The following solid–solid reaction between Li_2O and nanostructured metals may be kinetically limited, resulting in large hysteresis of voltage plateau. In the discharged state, the nanostructured metals are fully oxidized to form nanostructured metal oxide. In a complete charge–discharge cycle, bulk metal oxides transform to nanostructured ones, which can be referred as the electrochemical pulverization process.

In this work, it is intended to have discrete nanoparticles for investigating the difference between internally nanostructured

* Corresponding authors. Tel.: +886 2 27376624.
E-mail addresses: mycheng@mail.ntust.edu.tw, d8906107@mail.ntust.edu.tw (M.-Y. Cheng), bjh@mail.ntust.edu.tw (B.-J. Hwang).

0378-7753/$ – see front matter © 2013 Elsevier B.V. All rights reserved.
http://dx.doi.org/10.1016/j.jpowsour.2013.12.037

electrode (after 1st charge process of large-sized particles) and originally nanostructured electrode. It is expected the originally nanostructured electrode would not undergo electrochemical pulverization since their size scale is close to micro-sized one after 1st discharge and charge process (internally nanostructured metal oxide). The resulting stable electrode micro-/nano-structure for the originally nanostructured electrode may have significant effect to its hysteresis loop.

2. Experimental

To examine the difference, NiO is employed for illustration. Sub-micro-sized and nano-sized NiO particles are prepared to develop the internally nanostructured electrode and original nano-structured one, respectively. The discrete nano-sized NiO particles (referred as Nano-NiO) are prepared with confined synthesis developed in our previous work [16]. The process includes preparation of ordered mesoporous silica host, inclusion of Nano-NiO, and silica host removal, and is described in the following paragraphs.

SBA-15 is selected as the ordered mesoporous silica host, and the standard preparation conditions follow Zhao's work [17]. All chemicals were purchased from Acros (except P-123 from Sigma–Aldrich) and used as-received. For a standard process, 8.5 g of tetraethylorthosilicate (TEOS, 98%) 30 mL de-ionized H_2O were well mixed with 120 mL of 2 N HCl aqueous solution. The step was lasted for 20 h at 308 K. Later, the solution was sealed and statically aged at 373 K for 24 h. The resulting white precipitate was rinsed with de-ionized water and ethanol, and subsequently calcined at 823 K for 3 h. The obtained white powders are the said SBA-15.

For the synthesis of Nano-sized NiO in the pore channels of SBA-15, a modified hydrophobic encapsulation route was used [16]. The precursor solution was prepared with nickel nitrate hexahydrate (99 wt%, 0.035 mol) and citric acid (0.0175 mol) in de-ionized water (20 g). 1 g of SBA-15 was added to the precursor solution with continuous stirring and ultrasonic treatment to ensure complete impregnation of the precursor solution into the pore channels. The mixture was stirred and slowly heated at 60 °C for gradual inclusion of precursor until complete removal of bulk water. The dried powders were heated at a ramping rate of 5 °C min^{-1}–600 °C with further treatment at 600 °C for 1 h.

To release Nano-NiO from the SBA-15, the prepared materials were treated with 100 mL of 2 M NaOH (>99%, ACROS) solution ($EtOH:H_2O$ = 1:1 in vol%) to dissolve the silicate-based SBA-15. After 2 h-dissolution process, Nano-NiO was collected by vacuum filtration with microporous membrane (PVDF membrane filter, pore size: 0.2 μm, PALL). The solids were filtered, rinsed with de-ionized water for several times and dried in the oven at 80 °C.

For synthesis of sub-micron-sized NiO, 0.03 mol $Ni(NO_3)_2 \cdot 6H_2O$ (ACROS) was dissolved in 50 mL de-ionized water. Meanwhile, 0.12 mol NaOH was dissolved in 50 mL de-ionized water followed by dropping into a $Ni(NO_3)_2$ solution to form green precipitates. The precipitates were filtered and washed with de-ionized water for several times and dried at 80 °C. Finally the precipitates were heated at 600 °C for 1hr as the sub-micron-sized NiO (SubM-NiO).

The materials were characterized by XRD, TEM, BET, and TGA. For XRD patterns, a Rigaku D/Max-RC (Japan) diffractometer was operated at 40 kV and 100 mA with a Cu Kα radiation source. Bright-field TEM image was obtained with JEOL JEM-2010 microscope (Japan) with an accelerating voltage of 200 kV. For characterization of aged materials, the cycled cell was disassembled and the materials were scraped from anode active material layer. The scraped materials were rinsed with DEC solvent several times for removal of $LiPF_6$. Multi-point BET surface area was obtained by nitrogen adsorption technique with a Quantachrome AUTOSORB-1 at 77 K in liquid nitrogen bath. TGA was characterized for the cycled anode material of the aged half cell. The cycled anode material was scraped from the anode of the disassembled aged cell (with half cell charged to 3.0 V). The scraped material was rinsed with DEC (diethyl carbonate) several times to eliminate $LiPF_6$. TGA is performed with a ramping rate of 5 °C min^{-1} to a final temperature of 900 °C under flowing air with a rate of 20 mL min^{-1}.

The electrochemical performance of the materials was evaluated with coin cells using Li foil (FMC) as the anode and the fabricated electrode as the cathode. The anode and cathode were separated by a polypropylene separator saturated with 1 M $LiPF_6$ EC (ethylene carbonate)–DEC (diethyl carbonate) electrolyte solution (Tomiyama, EC:DEC = 1:1 in vol%). The fabricated electrode was prepared with slurry-casting method on the Cu foil. The electrode slurry was composed of active material (SubM-NiO or Nano-NiO), PVDF binder (polyvinylidene difluoride, 99%, ACROS) and carbon black (Super-P, Timcal) with a weight ratio of 6:2:2 in NMP (*N*-methyl-2-pyrrolidone, 99.5%, ACROS). The cast Cu foil was then dried in vacuum oven at 120 °C for 6 h. The dried foil was punched into numerous disks of 13 mm in diameter for the electrochemical testing. The active material was about 1 mg for each half cell. The assembled coin cell is galvanostatically cycled between 3 and 0.01 V at a constant C-rate of 0.2C. At the charge voltage of 3 V, the charge mode shifted to constant voltage until the charge current down to 0.05C. Coin cells were used for cyclic voltammetry (CV) and electrochemical impedance spectroscopy (EIS) as well. CV was performed in a potential window of 0.010–3.500 V with a scanning rate of 5 mV min^{-1} for 10 cycles. EIS was acquired at fully charged state of the half cell (in the state of NiO) during CV. The frequency ranges from 10^6 to 10^{-1} Hz with a DC interrupt of 10 mV. The as-assembled state was characterized as well.

3. Results and discussion

Firstly the XRD patterns for Nano-NiO and SubM-NiO are shown in Fig. 1. It is found that the peak broadening characteristic of fcc NiO (JCPDS - ICDD: 38-0715) is shown for Nano-NiO, indicating the nano-sized feature remaining before and after releasing process. For SubM-NiO, the same crystalline structure as Nano-NiO is shown except sharp peak feature in the XRD pattern. The Scherrer equation is adopted for calculation of the averaged grain size with FWHM (full width at half maximum) of the (2 0 0) peak. The averaged grain size for SBA-15-confined Nano-NiO is as small as

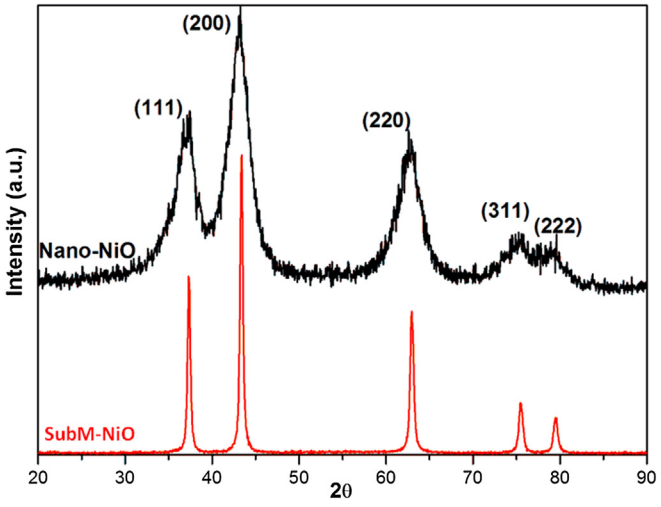

Fig. 1. XRD patterns of Nano-NiO and SubM-NiO.